NEW APPROACH IN DETERMINING THE TUNNELING COEFFICIENT FOR A TRIANGULAR BARRIER IN MIM JUNCTIONS

Emilia-Simona Mălureanu

Quantum tunneling has many important applications in electronics. In thin layers structures, when the tunneling phenomenon occurs at the metal-insulator contact barrier, as for the MIM or MOS structures, there is a Fowler-Nordheim field emission. In such structures, the tunneling currents must be calculated. The current density is calculated based on the transmission coefficient through the barrier, which is determined by solving the Schrödinger equation. The calculation methods currently used lead to values that get predictions of the tunneling current too low comparing to the experimental values. The transmission coefficient is calculated using harmonic wavelets and the results are validated experimentally on a MOM junction.

Keywords: Schrödinger equation, transmission coefficient, tunneling current

1. Introduction

As feature sizes of modern devices plunge beyond the submicron regime, quantum effects begin to play a more prominent role in governing the behavior of the devices.

This is the case of quantum tunneling phenomenon, with many important applications as cold emission, tunnel diode, transistors, scanning tunneling microscope, but also with undesired potential effects, mentioning the MOSFET, where the quantum tunneling represent a limitation regarding its design. The phenomenon appears in high intensity electric fields, around $1000kV/mm$.

In the case of MIM structures with a dielectric thickness of a few nanometers, conduction can occur in two ways.

At high temperatures and electric field strengths smaller than $10^8V/m$, the electrons, due to increased thermal agitation, gain enough energy to climb the potential barrier that occurs at metal-insulator interface. This conduction mechanism is called Schottky injection.

At normal temperatures and an electric field intensity that exceeds $10^8V/m$, the potential barrier, corresponding to the metal-insulator contact becomes very thin and there will appear the quantum type phenomenon called tunneling, when

Electrical Engineering Faculty, Numerical Methods Lab., POLITEHNICA University of Bucharest, Romania, e-mail: simona@lmn.pub.ro

electrons, although they do not have enough energy to climb the potential barrier, they manage to pass through the barrier. When the tunneling phenomenon occurs in metal-insulator contact barrier, this is a Fowler - Nordheim injection. In the case of devices that are based on the phenomenon of Fowler - Nordheim injection, the emission density current must be determined.

In thin layer structures, where the conduction is achieved by tunneling the barrier, the waves associated to the electrons suffer reflection from passing through the barrier. The current density will be calculated according to the barrier transmission coefficient, meaning the probability that the incident electrons to pass through the barrier. The quantum mechanical reflection can limit the current gain for these structures, so it is important for the optimal device design to know the extent of this reflection.

The transmission coefficient is determined by solving the Schrödinger equation. The exact calculation of the current density depends on the form of the potential barrier, but the existing methods for solving the Schrödinger equation lead to values that get predictions of the emission current density too low by a factor of 100 or more [1]. The triangular potential barrier is the most used in determining the tunneling current. The Schrödinger equation for this type of barrier is solved by WKB approximation, but this method has some drawbacks as not taking into account the wavefunction interference and, applied to the Fowler - Nordheim injection, it also does not consider the thickness of the insulator. This paper proposes a wavelet based method for solving the 1D Schrödinger equation for a triangular barrier and determining the transmission coefficient using the harmonic multiresolution analysis. The transmission coefficient is finally used to compute the emission current density and the theoretical results are compared afterwards to the experimental ones. The harmonic and Shannon wavelet methods were before applied by Bibic and Malureanu [2] in determining the transmission coefficient for a rectangular potential barrier.

Also, Malureanu and Craciunoiu [3] applied a wavelet based numerical method for determining the transmission coefficient.

2. **Rectangular potential barrier**

Let the one-dimensional time independent Schrödinger equation be considered

$$-\frac{h^2}{2m}\frac{\mathrm{d}^2\psi}{\mathrm{d}x^2} + U(x)\psi(x) = w\psi(x), \tag{1}$$

where the potential energy $U(x)$ is by the form

$$U(x) = \begin{cases} \mathbf{U_0} & , \ 0 \le x \le a \\ 0 & , \ \text{otherwise} \end{cases}, \ \mathbf{U_0} > 0\,, \tag{2}$$

and $\hbar$ represents Planck's constant divided by 2π, m represents the electron rest mass, ψ is the wave function, w is the total energy of the particle.

For $U(x) = 0$ the solution of (1) is

$$\psi(x) = k_1 \exp^{ix\sqrt{\frac{2mw}{\hbar^2}}} + k_2 \exp^{-ix\sqrt{\frac{2mw}{\hbar^2}}}, \tag{3}$$

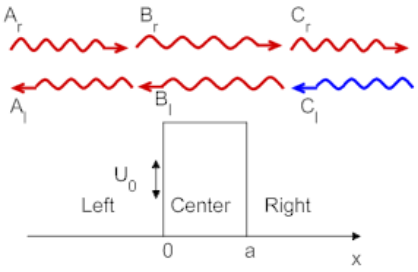

FIGURE 1. Rectangular potential barrier.

and (3) can be detailed as following.

Considering $k_0 = \sqrt{\frac{2mw}{\hbar^2}}$, then

$$\psi_L(x) = A_r \exp^{ik_0 x} + A_l \exp^{-ik_0 x}, \quad \text{if } x < 0\,, \tag{4}$$

and

$$\psi_R(x) = C_r \exp^{ik_0 x} + C_l \exp^{-ik_0 x}, \quad \text{if } x > a\,. \tag{5}$$

If $U(x) = \mathbf{U_0}$ $(w < \mathbf{U_0})$, then (1) becomes

$$\frac{\mathrm{d}^2\psi}{\mathrm{d}x^2} - k^2\psi(x) = 0\,, \tag{6}$$

where $k^2 = \frac{2m(U_0 - w)}{\hbar^2}$.

In this case, the solution has the form

$$\psi_C(x) = B_r \exp^{kx} + B_l \exp^{-kx}\,. \tag{7}$$

Applying the boundary conditions to (4),(5) and (7), the coefficients $A_{r,l}, B_{r,l}, C_{r,l}$ can be determined [4]. Two sets of conditions will be used

i) for $x = 0$

$$\begin{aligned} \psi_L(0) &= \psi_C(0), \\ \psi_L'(0) &= \psi_C'(0). \end{aligned} \tag{8}$$

ii) for $x = a$

$$\begin{aligned} \psi_C(a) &= \psi_R(a), \\ \psi_C'(a) &= \psi_R'(a)\,. \end{aligned} \tag{9}$$

The boundary conditions give the following restrictions on the coefficients

$$\begin{cases} A_r + A_l = B_r + B_l, \\ ik_0(A_r - A_l) = ik(B_r - B_l), \\ B_r \exp^{ika} + B_l \exp^{-ika} = C_r \exp^{ik_0 a} + C_l \exp^{-ik_0 a}, \\ ik(B_r \exp^{ika} - B_l \exp^{-ika}) = ik_0(C_r \exp^{ik_0 a} - C_l \exp^{-ik_0 a}) \end{cases} \tag{10}$$

To study the case of quantum tunneling, let us consider the following situation: a particle incident on the barrier from the left side (A_r) (see Fig.1). It may be either reflected (A_l) or transmitted (C_r). To find the amplitudes for reflection and

transmission for incidence from the left, we put in the above equations $A_r = 1$ (incoming particle), $A_l = r$ (reflection), $C_l = 0$ (no incoming particle from the right), and $C_r = t$ (transmission). We then eliminate the coefficients B_l, B_r from the equation and solve for r and t.

The reflection and transmission coefficient are

$$R = |r|^2 \ , \ T = |t|^2 \tag{11}$$

with

$$T = \frac{16{k_0}^2k^2}{({k_0}^2 + k^2)^2} \exp^{-2ka}, \tag{12}$$

and

$$R + T = 1. \tag{13}$$

This method applies only to constant coefficients Schrödinger equation so, only when the potential U, is constant.

3. **Triangular potential barrier**

This algorithm can be applied to more complex potential barrier types such as triangular potential barrier. The most used method to solve the Schrödinger equation for a triangular potential barrier is the WKB approximation. The approximate solution of the wavefunction according to WKB is [6]

$$\psi(x)_{WKB} \approx \exp\left[-\int_{x_1}^{x_2} k(x)\mathrm{d}x\right], \tag{14}$$

where

$$k(x) = \left[\frac{2m_0}{\hbar^2}(U(x) - w)\right]^{\frac{1}{2}}, \tag{15}$$

for

$$U(x) = w_F + \phi - q_0 \cdot E \cdot x. \tag{16}$$

$U(x)$ represents the triangular potential barrier, w_F = Fermi energy, ϕ =unreduced height of the barrier (zero field height), q_0 = elementary charge absolute value, E = intensity of the electric field. Considering a physical situation of an $Al - SiO_2 - Al$ sandwich, the values of the above physical quantities are $\phi = 3.2eV$, $q_0 = 1.6 \cdot 10^{-19}C$, $m_0 = 9.11 \cdot 10^{-31}kg$, $E = 10^9V/m$, $m_{ox} = 0.5 \cdot m_0kg$. The thickness of the insulator is $950\mathring{A}$, so in this case there will be a Fowler-Nordheim tunneling, characterizing thick layers ([5]). The total energy w of the electron is assumed to be equal to the Fermi energy w_F, so

$$k(x) = \left[\frac{2m_0}{\hbar^2}(\phi - q_0 \cdot E \cdot x)\right]^{\frac{1}{2}}. \tag{17}$$

In order to calculate the transmission coefficient, the value of the wavefunction in $[x_1, x_2]$ interval must be determined. In the WKB approximation, the coordinates x_1 and x_2 represent turning points, where the total energy is equal to the potential

energy of the particle. Considering that $U(x) - w = 0$, the integration limits x_1 and x_2 for (14) are determined

$$\begin{aligned} x_1 &= 0, \\ x_2 &= \frac{\phi}{q_0 \cdot E}. \end{aligned} \tag{18}$$

According to (17), the expression of the wavefunction in $[0, x_2]$ is

$$\psi = \exp\left[-\left(\frac{2m_0}{\hbar^2}\right)^{\frac{1}{2}} \cdot \frac{1}{q_0 \cdot E} \cdot \frac{2}{3} \cdot \phi^{\frac{3}{2}} \right]. \tag{19}$$

The transmission coefficient, according to (19), is

$$T = \psi \cdot \bar{\psi} = \exp(-2\int_{x_1}^{x_2} \sqrt{K(x)}\mathrm{d}x) = \exp\left(-\frac{4}{3}\left(\frac{2m_0}{\hbar^2}\right)^{\frac{1}{2}} \frac{\phi^{\frac{3}{2}}}{q_0 \cdot E} \right). \tag{20}$$

Considering the physical quantities that characterize the $Al - SiO_2 - Al$ structure, the value of the transmission coeficient according to (20) is

$$T = 9.33 \cdot 10^{-13}. \tag{21}$$

4. **The wavenumber as a function of frequency**

Considering the case when $U(x) = \mathbf{U_0}$ $(w < \mathbf{U_0})$, with

$$\frac{\mathrm{d}^2\psi}{\mathrm{d}x^2} - k^2\psi(x) = 0\,, \tag{22}$$

where

$$K(x) = k^2 = \frac{2m(U_0 - w)}{\hbar^2}. \tag{23}$$

Let

$$\psi(x) = \alpha\varphi(x) + \bar{\alpha}\bar{\varphi}(x) + \beta\eta(x) + \bar{\beta}\bar{\eta}(x), \tag{24}$$

the harmonic wavelet series expansion of (22) is

$$\alpha\frac{\mathrm{d}^2\varphi}{\mathrm{d}x^2} + \bar{\alpha}\frac{\mathrm{d}^2\bar{\varphi}}{\mathrm{d}x^2} + \beta\frac{\mathrm{d}^2\eta}{\mathrm{d}x^2} + \bar{\beta}\frac{\mathrm{d}^2\bar{\eta}}{\mathrm{d}x^2} - K(x)\cdot(\alpha\varphi(x) + \bar{\alpha}\bar{\varphi(x)} + \beta\eta(x) + \bar{\beta}\bar{\eta}(x)) = 0\,, \tag{25}$$

where α and β represent the harmonic wavelet coefficients, $\bar{\alpha}$ and $\bar{\beta}$ represent their conjugates, $\varphi(x)$ and $\eta(x)$ represent the harmonic scaling function and harmonic wavelet function, respectively, $\bar{\varphi}(x)$ and $\bar{\eta}(x)$ are their conjugates. The harmonic scaling function or "father wavelet" ([7]), is a complex function and has the following form

$$\varphi : \mathbb{R} \to \mathbb{C} \quad , \quad \varphi(x) \stackrel{def}{=} \begin{cases} \frac{\mathrm{e}^{2\pi i x} - 1}{2\pi i x}, & \text{if} \quad x \neq 0 \\ \\ 1, & \text{if} \quad x = 0. \end{cases} \tag{26}$$

The harmonic wavelet function, also named "mother wavelet" ([7]), is a complex valued function,having the following form

$$\eta : \mathbb{R} \to \mathbb{C} \quad , \quad \eta(x) \overset{def}{=} \begin{cases} \frac{e^{4\pi ix} - e^{2\pi ix}}{2\pi ix}, & \text{if} \quad x \neq 0 \\ \\ 1, & \text{if} \quad x = 0. \end{cases} \tag{27}$$

The following equalities are true (see [8])

$$\begin{aligned} &\frac{d^s}{dx^s}\left(\varphi(x)\right) = \lambda^{(s)}\varphi(x), \\ &\frac{d^s}{dx^s}\left(\eta(x)\right) = \gamma^{(s)}\eta(x)\,, \\ &\frac{d^s}{dx^s}\left(\bar{\varphi}(x)\right) = \bar{\lambda}^{(s)}\varphi(\bar{x}), \\ &\frac{d^s}{dx^s}\left(\bar{\eta}(x)\right) = \bar{\gamma}^{(s)}\bar{\eta}(x)\,, \end{aligned} \tag{28}$$

where λ and γ represent the connection coefficients of the scaling function and of the wavelet function respectively and $\bar{\lambda}$, $\bar{\gamma}$ represent their conjugates. Harmonic scaling function $\varphi(x)$, harmonic wavelet function $\eta(x)$ and their conjugates must satisfy the following(see [2])

$$\begin{cases} \left\langle \varphi^{HW}, \varphi^{HW} \right\rangle = \left\langle \bar{\varphi}^{HW}, \bar{\varphi}^{HW} \right\rangle = \left\langle \eta^{HW}, \eta^{HW} \right\rangle = \left\langle \bar{\eta}^{HW}, \bar{\eta}^{HW} \right\rangle = 1 \\ \left\langle \varphi^{HW}, \bar{\varphi}^{HW} \right\rangle = \left\langle \bar{\varphi}^{HW}, \varphi^{HW} \right\rangle = \left\langle \eta^{HW}, \bar{\eta}^{HW} \right\rangle = \left\langle \bar{\eta}^{HW}, \eta^{HW} \right\rangle = 0 \\ \left\langle \varphi^{HW}, \eta^{HW} \right\rangle = \left\langle \eta^{HW}, \varphi^{HW} \right\rangle = \left\langle \bar{\varphi}^{HW}, \bar{\eta}^{HW} \right\rangle = \left\langle \bar{\Psi}^{HW}, \bar{\varphi}^{HW} \right\rangle = 0 \\ \left\langle \varphi^{HW}, \bar{\eta}^{HW} \right\rangle = \left\langle \bar{\eta}^{HW}, \varphi^{HW} \right\rangle = \left\langle \bar{\varphi}^{HW}, \eta^{HW} \right\rangle = \left\langle \eta^{HW}, \bar{\varphi}^{HW} \right\rangle = 0\,. \end{cases} \tag{29}$$

Considering (28), equation (25) becomes

$$\alpha\lambda^{(2)}\varphi(x)+\bar{\alpha}\bar{\lambda}^{(2)}\bar{\varphi}(x)+\beta\gamma^{(2)}\eta(x)+\bar{\beta}\bar{\gamma}^{(2)}\bar{\eta}(x)-K(x)\cdot(\alpha\varphi(x)+\bar{\alpha}\bar{\varphi}(x)+\beta\eta(x)+\bar{\beta}\bar{\eta}(x)) = 0\,. \tag{30}$$

The projection of (22) in a dimensional finite wavelet space $\Pi^{N,M}$ verifies (see [8])

$$\begin{aligned} &\left\langle \Pi^{N,M}\left[\frac{d^2}{dx^2}\left(\psi(x)\right)\right], \varphi(x)\right\rangle - \left\langle \Pi^{N,M}\left[K(x)\right], \varphi(x)\right\rangle \cdot \left\langle \Pi^{N,M}\left[\psi(x)\right], \varphi(x)\right\rangle = 0\,, \\ &\left\langle \Pi^{N,M}\left[\frac{d^2}{dx^2}\left(\psi(x)\right)\right], \eta(x)\right\rangle - \left\langle \Pi^{N,M}\left[K(x)\right], \eta(x)\right\rangle \cdot \left\langle \Pi^{N,M}\left[\psi(x)\right], \eta(x)\right\rangle = 0\,, \\ &\left\langle \Pi^{N,M}\left[\frac{d^2}{dx^2}\left(\psi(x)\right)\right], \varphi(\bar{x})\right\rangle - \left\langle \Pi^{N,M}\left[K(x)\right], \varphi(\bar{x})\right\rangle \cdot \left\langle \Pi^{N,M}\left[\psi(x)\right], \varphi(\bar{x})\right\rangle = 0\,, \\ &\left\langle \Pi^{N,M}\left[\frac{d^2}{dx^2}\left(\psi(x)\right)\right], \eta(\bar{x})\right\rangle - \left\langle \Pi^{N,M}\left[K(x)\right], \eta(\bar{x})\right\rangle \cdot \left\langle \Pi^{N,M}\left[\psi(x)\right], \eta(\bar{x})\right\rangle = 0\,. \end{aligned} \tag{31}$$

For $\forall\, s \in \mathbb{N}$

$$\begin{aligned} \bar{\lambda}^{(s)} &= (-1)^s \lambda^{(s)}\,, \\ \bar{\gamma}^{(s)} &= (-1)^s \gamma^{(s)}\,. \end{aligned} \tag{32}$$

Considering(29), (31) and (32), by inner product with $\varphi(x)$, $\eta(x)$ and their conjugates, the following system of equations is obtained from (30)

$$\begin{cases} \alpha\lambda^{(2)} - \langle K(x),\, \varphi(x)\rangle \cdot \alpha = 0 \\ \\ \beta\gamma^{(2)} - \langle K(x),\, \eta(x)\rangle \cdot \beta = 0 \\ \\ \bar{\alpha}\lambda^{(2)} - \left\langle K(x),\, \varphi(\bar{x})\right\rangle \cdot \bar{\alpha} = 0 \\ \\ \bar{\beta}\gamma^{(2)} - \left\langle K(x),\, \eta(\bar{x})\right\rangle \cdot \bar{\beta} = 0 \end{cases} \tag{33}$$

The following notation is proposed

$$\begin{aligned} b = \langle K(x),\, \varphi(x)\rangle\,, c = \langle K(x),\, \eta(x)\rangle\,, \\ d = \left\langle K(x),\, \varphi(\bar{x})\right\rangle, e = \left\langle K(x),\, \eta(\bar{x})\right\rangle. \end{aligned} \tag{34}$$

The values of the connection coefficients for this case are $\lambda^{(2)} = -\frac{\pi^2}{3}$ şi $\gamma^{(2)} = 0$ (see [9]).

According to Parceval equality

$$\langle f(x), g(x)\rangle = \frac{1}{2\pi}\left\langle \widehat{f}(\omega), \widehat{g}(\omega)\right\rangle = \frac{1}{2\pi}\int_{\mathbb{R}} \left|\widehat{f}(\omega)\cdot\widehat{g}(\omega)\right| \mathrm{d}\omega\,, \tag{35}$$

$$\langle f(x), \bar{g}(x)\rangle = \frac{1}{2\pi}\left\langle \widehat{f}(\omega), \overline{\widehat{g}(-\omega)}\right\rangle = \frac{1}{2\pi}\int_{\mathbb{R}} \left|\widehat{f}(\omega)\cdot\overline{\widehat{g}(-\omega)}\right| \mathrm{d}\omega\,. \tag{36}$$

The Fourier transform of $\varphi(x)$ function is ([9])

$$\widehat{\varphi}(\omega) = \chi(\omega + 2\pi) = \begin{cases} 1, & \text{if} \quad 0 \le \omega \le 2\pi \\ \\ 0, & \text{otherwise,} \end{cases} \tag{37}$$

where

$$\chi\,(\omega) = \begin{cases} 1, & \text{if} \quad 2\pi \le \omega \le 4\pi \\ \\ 0, & \text{otherwise} \end{cases} \tag{38}$$

represents "the characteristic function" (or "box").

In the first equation of the system (33)

$$\begin{aligned} b = \frac{1}{2\pi}\left\langle \widehat{K}(\omega),\, \hat{\varphi}(\omega)\right\rangle = \frac{1}{2\pi}\int_{\mathbb{R}} \left|\widehat{K}(\omega)\cdot\widehat{\varphi}(\omega)\right| \mathrm{d}\omega = \\ = \frac{1}{2\pi}\int_0^{2\pi} \widehat{K}(\omega)\mathrm{d}\omega\,, \end{aligned} \tag{39}$$

where $\widehat{K}(\omega)$ represents the Fourier transform of the (23) function. Also, according to Parceval equality, and considering that the Fourier transform of $\eta(x)$ is

$$\widehat{\eta}(\omega) = \chi(\omega), \tag{40}$$

where

$$\chi(\omega) = \begin{cases} 1, & \text{if} \quad 2\pi \leq \omega \leq 4\pi \\ \\ 0, & \text{otherwise,} \end{cases} \tag{41}$$

represents "the characteristic function" (or "box"), in the second equation of the system (33)

$$\begin{aligned} c = \frac{1}{2\pi}\left\langle \hat{K}(\omega),\, \hat{\eta}(\omega)\right\rangle = \frac{1}{2\pi}\int_{\mathbb{R}} \left|\widehat{K}(\omega)\cdot\widehat{\eta}(\omega)\right| d\omega = \\ = \frac{1}{2\pi}\int_{2\pi}^{4\pi} \widehat{K}(\omega)\mathrm{d}\omega\,. \end{aligned} \tag{42}$$

Using the Fourier property that

$$\mathcal{F}\left[\bar{f}(x)\right] = \overline{\widehat{f}(-\omega)}\,, \tag{43}$$

the Fourier transforms of the scaling and wavelet functions conjugates are determined(see [2])

$$\widehat{\bar{\varphi}}(\omega) = \chi\left(\omega + 4\pi\right) \tag{44}$$

$$\widehat{\bar{\eta}}(\omega) = \chi\left(\omega + 6\pi\right)\,. \tag{45}$$

Considering (44), (45) and Parceval equality

$$\begin{aligned} d = \frac{1}{2\pi}\left\langle \widehat{K}(\omega),\, \overline{\widehat{\varphi}(\omega)}\right\rangle = \frac{1}{2\pi}\int_{\mathbb{R}} \left|\widehat{K}(\omega)\cdot\overline{\widehat{\varphi}(\omega)}\right| \mathrm{d}\omega = \\ = \frac{1}{2\pi}\int_{-2\pi}^{0} \widehat{K}(\omega)\mathrm{d}\omega\,, \end{aligned} \tag{46}$$

$$\begin{aligned} e = \frac{1}{2\pi}\left\langle \hat{K}(\omega),\, \hat{\eta}(\omega)\right\rangle = \frac{1}{2\pi}\int_{\mathbb{R}} \left|\widehat{K}(\omega)\cdot\widehat{\eta}(\omega)\right| d\omega = \\ = \frac{1}{2\pi}\int_{-4\pi}^{-2\pi} \widehat{K}(\omega)\mathrm{d}\omega\,. \end{aligned} \tag{47}$$

Solving the integrals(39), (42), (46), (47), the sum $|b|+|d|$ will be always equal to the square of the wavenumber, k^2, and $c = e = 0$. In order to verify this, the harmonic wavelet solution was compared to the analytical solution for a rectangular potential barrier. Also, the free electron model case was considered, comparing the wavelet solution to analytically obtained k_0^2. the results are presented in the tables below (Tables 1, 2). Let the harmonic wavelet algorithm be applied on the above

TABLE 1. k^2 and $|b| + |d|$ for different values of U_0 and w

	$U_0 = 5$, $w = 4$	$U_0 = 7$, $w = 5$	$U_0 = 10$, $w = 6$
k^2	4.2082	8.4164	16.8328
$\|b\| + \|d\|$	4.2082	8.4164	16.8328

TABLE 2. k_0^2 and $|b| + |d|$ for different values of w

	$w = 2$	$w = 5$	$w = 7$
k_0^2	8.4164	21.041	29.457
$\|b\| + \|d\|$	8.4164	21.041	29.457

triangular potential barrier. The result is

$$\begin{aligned} |b| &= \frac{1}{2\pi}\int_0^{2\pi} \widehat{K}(\omega)\mathrm{d}\omega = 10.02, \\ |d| &= \frac{1}{2\pi}\int_{-2\pi}^{0} \widehat{K}(\omega)\mathrm{d}\omega = 10.02, \\ |b| + |d| &= 20.04\,. \end{aligned} \tag{48}$$

Considering that $\frac{1}{2\pi}\int_0^{2\pi} \widehat{K}(\omega)\mathrm{d}\omega + \frac{1}{2\pi}\int_{-2\pi}^{0} \widehat{K}(\omega)\mathrm{d}\omega = |b| + |d| = K(x)$ is a constant, it means that the time independent Schrödinger equation for a triangular potential barrier can be solved by the analytical method described in (2) as a equation with constant coefficients.

Considering the analytical expresion of the transmission coefficient

$$T_{an} = \frac{16{k_0}^2|b| + |d|}{({k_0}^2 + |b| + |d|)^2}\exp^{-2\sqrt{|b|+|d|}a}, \tag{49}$$

and replacing k with $\sqrt{|b| + |d|}$, the result for the transmission coefficient through the barrier obtained is

$$T^{\mathrm{HW}} = 2.94 \cdot 10^{-12}, \tag{50}$$

with $a = 1.52$ coresponding to the thickness of the insulator $(950\mathring{A})$ for fields up to $10^9 V/m$ [10].

5. **Tunneling current**

The tunneling current is given by

$$I = \frac{\pi r^2}{2} \cdot j, \tag{51}$$

where r represents the radius of the emission electrode and j is the density current.

The calculation of the current density for the Fowler-Nordheim emission is made according to the following equation

$$j = M \cdot E^2 \cdot \exp(-\frac{B}{E}), \tag{52}$$

where

$$M = \frac{q_0^3 m_0}{16\pi\hbar m_{ox}\phi} = 1.54 \cdot 10^{-6} \frac{m_0}{m_{ox}} \cdot \frac{1}{\phi} (A/V^2). \tag{53}$$

The second part of the expression (52) represents the transmission coefficient

$$T = \exp(-\frac{B}{E}) = \psi \cdot \bar{\psi}, \tag{54}$$

where ψ represents the wave function. Considering the transmission coefficient determined for a triangular potential barrier with the harmonic wavelets (50), the current density, considering a physical situation of an $Al - SiO_2 - Al$ sandwich (see Section (3)), is

$$j = M \cdot E^2 \cdot \exp(-\frac{B}{E}) = 5.4 \cdot 10^{-6} \cdot 10^{18} \cdot 2.94 \cdot 10^{-12} = 15.87 \ (A/m^2) \,. \tag{55}$$

The value of the tunneling current, according to (51) and (55), is

$$I = 5.6 \cdot 10^{-11} A. \tag{56}$$

6. Experiments

6.1. Metal-oxide-metal tunnel junctions

The experimental validation of the theoretical results was made on $Al - SiO_2 - Al$ structures, which were specially designed and realised by silicon planar technology. The experimental part was conducted at National Institute for Research and Development in Microtechnologies from Bucharest.

Figure (2) presents a schematic view of such a structure and Figure (3) shows the optical and SEM microscope top view.

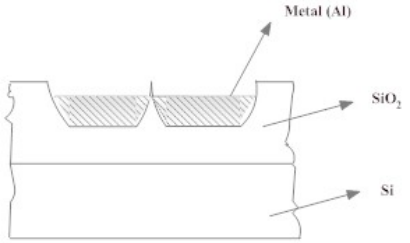

FIGURE 2. $Al - SiO_2 - Al$ sample schematic structure-cross section.

As can be seen in the images, the mentioned structure consists of two metal (Al) islands separated by a thin barrier wall of SiO_2. The SiO_2 barrier was obtained by corrosion of approximately half of the oxide layer, which initial thickness was $1.6\mu m$, through a photoresist mask, obtaining two cavities in the oxide, separated by a wall with a controlled thickness. The metal was deposited on the bottom of the cavities by lift-off technique. The SEM image for Figure (3b) presents the two metal arrays, separated by the oxide wall with its width at the level of the deposited metal of aproximately 90 nm.

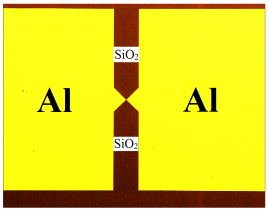

(A) Optic microscope view of the experimental junction.

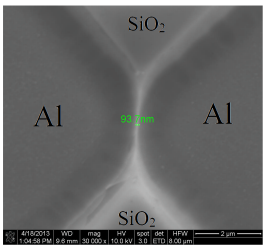

(B) Scanning electron microscope (SEM) view of the experimental junction.

FIGURE 3. $Al - SiO_2 - Al$ sample.

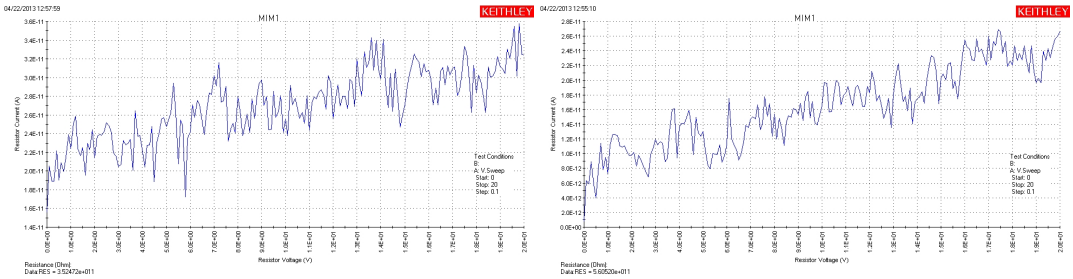

FIGURE 4. $I(U)$ diagram measurements for $Al - SiO_2$ junctions

6.2. Measurements

The measurements on the $Al-SiO_2$ junctions were made with Keithley Model-4200 SCS/C, EP6/ Suss MicroTec. Regarding the test conditions, the measurements were made at room temperature, applying a $0 - 20V$ input, with a 0.1 voltage increasing step. The peaks from Figure (4) indicate the Gundlach oscillations [11], attributed to the interference of the incident electron waves and electron waves which are reflected at the barrier-electrode interface. Also, the graphs show a growth of the current as a function of the input voltage, so as a function of the electric field intensity, aspect that verifies the Fowler-Nordheim tunneling. The measured tunneling currents have close values to the theoretical result.

This is a very good model for estimating the value of the tunneling current since the models based on the WKB approximation, like that proposed by Fowler and Nordheim [1], give a value for the tunneling current smaller with two orders of magnitude than the experiments.

7. Conclusions

The transmission coefficient has a great influence on the value of the tunneling current. The harmonic multiresolution analysis was used to calculate the transmission coefficient for a triangular potential barrier. The theoretical determined value

of the tunneling current was validated experimentally. The measurements show that the proposed method offers a good approximation of the the transmisssion coefficient and, as a result, of wave function. The transmission coefficient was used to calculate the current density and tunneling current. The results are in concordance with the experimental measured values.

The WKB method, which is usually used in tunneling problems, does not consider the thickness of the dielectric for thick layers $(5 - 100\text{nm})$. The wavelet based method offers the possiblility to consider the thickness of the dielectric, and this is the main reason for obtaining a better estimation than the WKB method of the transmission coefficient.

Acknowledgment

This work has been supported by the Sectorial Operational Programme Human Resources Development 2007-2013 of the Romanian Ministry of Labour, Family and Social Protection through the Financial Agreement POSDRU/107/1.5/S/76813.

REFERENCES

[1] R.H.Fowler and L. Nordheim. *Electron Emission in Intense Electric Fields*, Proceedings of the Royal Society of London , vol.119, pp. 173-181, 1928.

[2] S. Bibic and S. Malureanu. *Wavelet Solution of the Time Independent Schrödinger Equation for a Rectangular Potential barrier*, ATEE, 2013.

[3] S. Malureanu and F. Craciunoiu. *Wavelet Solution of the Schrdinger Equation for a Triangular Potential Barrier and applied results on a MOM tunnel junction*, International Semiconductor Conference, 2013.

[4] Eugen Merzbacher. *Quantum Mechanics* , Wiley, 3-rd edition, 1997.

[5] J.C. Ranuarez, M.J. Deen and C. Chen. *A review of gate tunneling current in MOS devices*,Microelectronics reliability, 46, 1939-1956, 2006.

[6] Mohsen Razavy. *Quantum Theory of Tunneling*. World Scientific, 1-st edition, 2003.

[7] D.E.Newland.*Harmonic wavelet analysis*, Proc.of the Royal Society of London, 443, pp. 203-225, 1993.

[8] C. Cattani. *Harmonic wavelet solution of Poisson's problem*, Balkan Journal of Geometry and Its Applications, **13**, 1, pp.27-37, 2008.

[9] C. Cattani. *Shannon Wavelet Theory*. Mathematical Problems in Engineering, pp. 1-24, 2008.

[10] B. Politzer. *Comparison of a Numerical Method and the WKB Approximation in the Determination of Transmission Coefficients for Thin Insulating Films*, Journal of Applied Physics, **37**, 279-286, 1966.

[11] K.H. Gundlach. *Zur Berechnung des Tunnelstroms durch eine trapezförmige Potentialstufe*, Solid-State Electron., **9**, 949957, 1966.